23rd IMEKO TC4 International Symposium
Electrical & Electronic Measurements Promote Industry 4.0
September 17-20, 2019，Xi'an, China

Microwave Characterization of 3D-printer Dielectric Materials

Andrea Alimenti[1], Kostiantyn Torokhtii[1], Nicola Pompeo[1], Emanuele Piuzzi[2] and Enrico Silva[1]

[1]Dipartimento di Ingegneria, Università degli Studi Roma Tre, 00146 Roma, Italy,
[2]Dipartimento di Ingegneria dell'Informazione, Elettronica e Telecomunicazioni, Sapienza Università di Roma, Roma, Italy,
mail: andrea.alimenti@uniroma3.it

***Abstract* – 3D-printer materials are becoming increasingly more appealing also for high frequency applications. Thus, the electromagnetic characterization of these materials is an important step in order to evaluate their applicability in new technological devices. We present a measurement method for the loss tangent evaluation based on a dielectric loaded resonator (DR). Comparing the quality factor Q of the DR with a disk-shaped sample placed on a DR base with Q obtained when the sample is substituted with an air gap, allows a reliable loss tangent determination.**

Keywords* – *microwave characterization, loss tangent, 3D-printer materials, dielectric resonator

I. INTRODUCTION

In the last years the fast development and improvement of 3D-print techniques have strongly affected many human activities [1-5]. Printed materials are also involved in high frequency applications as telecommunication technologies up to microwave frequencies [6-12]. Thus, a reliable and handy electromagnetic (e.m.) characterization is increasingly requested [13].

In this work we present the microwave characterization of plastic materials for 3D-printers with a resonant perturbative technique. The physical quantity under investigation is the permittivity $\boldsymbol{\varepsilon}$, which is defined as the quantity (in the more general case a tensor) which describes the proportionality between the electric displacement vector $\boldsymbol{D}$ and the electric field strength vector $\boldsymbol{E}$ in a medium, $\boldsymbol{D} = \varepsilon_0 \boldsymbol{\varepsilon} \cdot \boldsymbol{E}$. In our case we consider isotropic and homogeneous materials in their linear regime, then $\boldsymbol{\varepsilon} = \tilde{\varepsilon}$ is a scalar quantity which does not depend on the position. The scalar complex relative permittivity is defined as $\tilde{\varepsilon} = \varepsilon' + i\varepsilon''$, where the real part ε' is a measure of the energy storage properties of the medium while the imaginary part ε'' is related to the e.m. losses. Since $\tilde{\varepsilon}$ is a complex quantity, it is often represented on the complex plane, where the angle δ between $\tilde{\varepsilon}$ and the real axis is known as loss angle. Thus, the ratio $\varepsilon''/\varepsilon' = \tan\delta$ is called the loss tangent.

We propose in this work a measurement method based on a resonant technique. We show that a dielectric loaded resonator with an open base can be used to measure $\tilde{\varepsilon}$ by placing the dielectric sample on one of its flat bases, without the need for disassembling and reassembling the whole structure for each measurement, thus reducing the uncertainties involved.

Dielectric resonators are well known for their high sensitivity [14], but also for the poor measurement repeatability [15-16] in particular for what concerns the resonant frequency. Thus, a closed structure can be particularly useful to characterize samples by reducing systematic errors inevitably introduced by each mounting procedure. Moreover, since it is not necessary to reassemble the resonator for each measurement, the measurement time is reduced.

We substituted a part of the volume of the resonating structure with a different dielectric material. Comparison of the changes of the unloaded quality factor Q and the resonant frequency f_0 can be used to evaluate the electric/magnetic properties of the sample. If the changes on the distribution of the electromagnetic (e.m.) field caused by the insertion of the sample are "small", the resonant medium perturbation method [14] can be used.

Dielectric printed materials are already used for high frequency applications, and some works explored their dielectric constant. Noticeable is the result obtained in [17] where acrylonitrile butadiene styrene (ABS) doped with different quantities of $BaTiO_3$ microparticles, allowed to obtain $2.6 < \varepsilon' < 8.7$ and $0.005 < \tan\delta < 0.027$, thus opening the possibility to engineer these materials for specific needs. The measurements were performed at 15 GHz with a split post dielectric resonator, a very sensitive technique but critical for the resonator assembly procedure. With a combined technique, a broad band (1 MHz ÷ 11 GHz) characterization of 3D-printer materials was presented in [13]. The high frequency range (8.2 GHz ÷ 11 GHz) was studied through a Nicholson-

Ross-Weir waveguide in reflection mode, although an uncertainty study was lacking in this frequency range. Reported values at 11 GHz were $2.5 < \varepsilon' < 3.29$ and $0.005 < \tan\delta < 0.037$.

In fact, our resonator works at a similar frequency (~ 12.9 GHz), with a somewhat reduced sensitivity with respect to a split post resonator, but with much improved ease of operation, a useful feature in view of routine or mass measurements.

One should mention that the layered deposition techniques, typical of most of the 3D-printers, can generate anisotropic effects on the e.m. properties of the printed samples. It was measured a uniaxial anisotropy factor of almost 7 % on ε' at 40 GHz on polylactide (PLA) samples with waveguide reflection method [18]. In the method presented here the $\boldsymbol{E}$ field is almost parallel to the deposition layers of the sample, thus our results probe the direction along the layer deposition, without significant mixing of the perpendicular component.

In Sec. II we present an in-depth analysis of the measurement method, including a detailed evaluation of the measurement uncertainties. In Sec. III we present the experimental results. A short summary is presented in Sec IV.

II. DESCRIPTION OF THE METHOD

We use a special configuration of a dielectric loaded resonator in Hakki-Coleman [19] configuration, designed to guarantee enhanced measurement repeatability at room temperature. The two physical quantities that characterize the response of the resonator are the unloaded quality factor Q and the resonant frequency f_0. Q is defined as $Q = \omega_0 W/P$, where W is the energy stored into the resonator at the resonant angular frequency $\omega_0 = 2\pi f_0$ and P the power dissipated at the same frequency. Thus, as we will show below, we can obtain the information about the dielectric losses of the material under study (i.e. the $\tan\delta$), from a measurement of the Q.

P is the sum of all the power losses $P = P_S + P_\Omega + P_V$, where we indicate with the subscripts S, Ω, V the quantities related respectively to the sample, to the metal surfaces and to all the other dielectric materials inside the resonator volume. Hence:

$$\frac{1}{Q} = \frac{P_S + P_\Omega + P_V}{\omega_0 W} = \frac{1}{Q_S} + \frac{1}{Q_\Omega} + \frac{1}{Q_V}, \qquad (1)$$

with:

$$\frac{1}{Q_S} = \frac{\int_{V_S} \varepsilon_S'' \varepsilon_0 |\mathbf{E}|^2 \mathrm{dV}}{2\mathrm{W}} = \left[\frac{\varepsilon_S' \int_{V_S} \varepsilon_0 |\mathbf{E}|^2 \mathrm{dV}}{2\mathrm{W}}\right] \frac{\varepsilon_S''}{\varepsilon_S'} = \eta_S \tan\delta_S, \qquad (2)$$

$$\frac{1}{Q_\Omega} = \sum_i \frac{\int_{S_i} R_i |\boldsymbol{H}_\tau|^2 \mathrm{dS}}{2\mathrm{W}} = \sum_i \frac{R_i}{G_i}, \qquad (3)$$

$$\frac{1}{Q_V} = \frac{\int_{V_V} \varepsilon_V'' \varepsilon_0 |\boldsymbol{E}|^2 dV}{2W} = \eta_V \tan\delta_V, \qquad (4)$$

where $\boldsymbol{E}$ is the electric field and $\boldsymbol{H}_\tau$ is the magnetic field tangential to the metallic surfaces. η_S and η_V are the filling factors of the sample and of the dielectric elements inside the resonator respectively. R_i is the surface resistance R of the i-th surface with geometrical factor G_i. Thus:

$$\frac{1}{Q} = \eta_S \tan\delta_S + \sum_i \frac{R_i}{G_i} + \eta_V \tan\delta_V, \qquad (5)$$

Since W and the field configuration depend on ε' of all the dielectric elements inside the resonator, both η and G are functions also of ε_S'. Thus, to evaluate $\tan\delta_S$ of the dielectric sample placed in the resonator from Eq. (5), ε_S' must be measured. To this aim, one can exploit f_0 of the resonator as a second measurand. However, it is known that the absolute value of f_0 is strongly affected by many intrinsic (e.g. the electromagnetic properties of the elements inside the resonator) and extrinsic (e.g. temperature, pressure, humidity) factors, so that it is very difficult to exploit it in practice. However, the variation $\Delta f_0/f_{ref}$ of f_0 due to the changes in one or more parameters is much more reliable [14]. In our case, we measure Δf_0 caused by the insertion of the dielectric sample. Then, with electromagnetic simulations we calculate Δf_0 as a function of ε_S' until the simulated and measured Δf_0 coincide. Thus, ε_S' is evaluated with the aid of e.m. simulations of the resonator.

After that ε_S' is evaluated, the factors η and G in Eq. (5) can be analytically or numerically (with simulators) calculated. Then, Eq. (5) can be inverted to obtain $\tan\delta_S$ from Q measurements if all the R_i and $\tan\delta_V$ of the resonator are known from previous measurements or calibration procedures.

It must be mentioned that the unloaded Q in Eq. (5) differs from the measured Q_l because of the coupling of the resonator with the external lines. However, with very small coupling, as in our working condition, one has $Q_l \sim Q$ and $u(Q) \sim u(Q_l)$ [14].

The use of Eq. (5) can give unacceptably large uncertainties since at microwave frequencies, the accuracy with which all the quantities in Eq. (5) are known is poor if compared to dc or low frequency measurements. In fact, in our case, we have $R = 92$ mΩ with $u(R)/R \sim 15$ % and $\tan\delta_V = 4 \cdot 10^{-5}$ with $u(\tan\delta_V)/\tan\delta_V \sim 50$ %.

In order to reduce the contribution of these uncertainties on $\tan\delta_S$, we propose to use a perturbative approach. The difference $\Delta[Q^{-1}]$ between the measured quality factors Q_S^{-1} and Q_A^{-1}, obtained with the sample into the resonator (subscript S) or with a gap of air in its place (subscript A) respectively, can be written as:

$$\Delta[Q^{-1}] = \eta_S \tan\delta_S + \sum_i R_i \Delta[G_i^{-1}] + \Delta[\eta_V] \tan\delta_V \qquad (7)$$

where it is clear that the smaller $\Delta[G_i^{-1}]$ and $\Delta[\eta_V]$ are, then the smaller the uncertainties on R_i and $\tan\delta_V$ contributions are. In particular the overall uncertainty on $\tan\delta_S$ is [20]:

$$u^2(\tan\delta_S) = \frac{1}{\eta_S^2}\left[(u(\Delta[Q^{-1}])^2 + \sum_i\left(\Delta[G_i^{-1}]u(R_i)\right)^2 + \sum_i\left(R_i u(\Delta[G_i^{-1}])\right)^2 + (\tan\delta_V u(\Delta[\eta_V]))^2 + \left(\Delta[\eta_V]u(\tan\delta_V)\right)^2 + (\tan\delta_S u(\eta_S))^2\right], \quad (8)$$

with:

$$u^2(\Delta[Q^{-1}]) = \left(\frac{u(Q_S)}{Q_S^2}\right)^2 + \left(\frac{u(Q_A)}{Q_A^2}\right)^2 \quad (9)$$

$$u^2(\Delta[G_i^{-1}]) = \left(\frac{u(G_{i,S})}{G_{i,S}^2}\right)^2 + \left(\frac{u(G_{i,A})}{G_{i,A}^2}\right)^2 - 2r_G\frac{u(G_{i,S})u(G_{i,A})}{G_{i,S}^2 G_{i,A}^2} \quad (10)$$

$$u^2(\Delta[\eta_V]) = u^2(\eta_{V,S}) + u^2(\eta_{V,A}) - 2r_\eta u(\eta_{V,S})u(\eta_{V,A}) \quad (11)$$

The correlation factors r_G and r_η are supposed to be almost 1 since the evaluation of G_i and η_V is performed with the same algorithm and with the same settings. Instead, the Q measurements are not strongly correlated since the different mountings can give different uncorrelated error contributions.

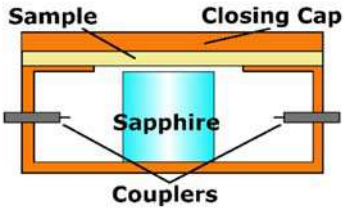

Figure 1- Sketch of the dielectric loaded resonator.

III. RESULTS AND DISCUSSIONS

The resonator used for this study is depicted in Figure 1. The dielectric samples are supported by the brass mask with a central hole $\varnothing = (13.00 \pm 0.01)$ mm and closed with a brass cap in order to prevent energy radiation. The measurements were performed on four dielectric samples, made all of the same dielectric material, and of different thickness values *t* as reported in Table 1. The thickness of the samples and their flatness were checked with a micrometer. The mean values $\bar{t}$ and their standard deviation $\sigma_t = \sqrt{\sum_{i=1}^{N}(t-\bar{t})^2/(N-1)}$ have been obtained by $N = 10$ different measurements of the thickness probing the surfaces of the samples. Thus, σ_t can be read as a measure of the flatness of the samples.

Table 1. The mean thickness $\bar{t}$ and its standard deviation σ_t

	S_1	S_2	S_3	S_4
$\bar{t}$ [mm]	0.522	1.002	1.512	2.063
σ_t [mm]	0.003	0.004	0.005	0.004

For each sample, the measurement is performed as follows:

- The Vector Network Analyzer (VNA) is calibrated with SOLT method and the 12-errors parameters are applied to the frequency range in which the measurements are performed;
- The transmission scattering parameter $S_{12}(f)$ is acquired with 1601 points evenly distributed in a frequency range width $7\Delta f_{-3dB}$, where Δf_{-3dB} is the width of the resonance curve at half power. Each data point is averaged with 10 acquisitions to reduce the noise contribution;
- The absolute value of the acquired points $|S_{12}(f)|$, with their uncertainty $u(S_{21}(f))$, given by the VNA after the calibration [21], are fitted to the Fano resonance curve [22,23]:

$$|S_{12}(f)| = \left|\frac{S_{12}(f_0)}{1+2iQ\frac{f-f_0}{f_0}} + \alpha + i\beta\right| \quad (12)$$

where the complex constant $\alpha + i\beta$ represents the cross-coupling contribution. For each resonance curve, Q and f_0 are evaluated with their uncertainties $u(Q)$, $u(f_0)$ obtained from the residuals of the fitting algorithm;
- For each mounting 10 resonance curves are acquired. Then, the mean values of Q and f_0 evaluated with their standard deviation are: $u(Q)/Q \sim 0.05\%$ and $u(f_0)/f_0 \sim 1$ ppm;
- For each sample 5 mountings are performed disassembling and resetting the sample in its position. Then, the mean value of Q and f_0 with their standard deviation are evaluated. The final uncertainties $u(Q)/Q \sim 1\%$ and $u(f_0)/f_0 \sim 20$ ppm are mainly due to the assembling repeatability.

A sensitive enough method to evaluate ε_r relies on the frequency repeatability of our setup, so that we can reliably measure the differences between $f_{0,S}$ measured with the dielectric samples mounted and $f_{0,A}$ measured without the sample and leaving an air gap of the same sample thickness. This is realized thanks to 3D-printed rings, prepared in the same way and of the same thickness of the dielectric samples. The data are presented in Figure 2: from those one can then evaluate $\varepsilon_{r,S} = 2.9 \pm 0.2$.

Once ε_r is estimated with its uncertainty, the

geometrical and filling factors of the resonator components are evaluated from the simulations. The uncertainties related to these quantities are obtained varying all the geometrical and electromagnetic quantities in the simulation in their confidence intervals, then the standard deviations of the simulated G and η are taken as their uncertainties.

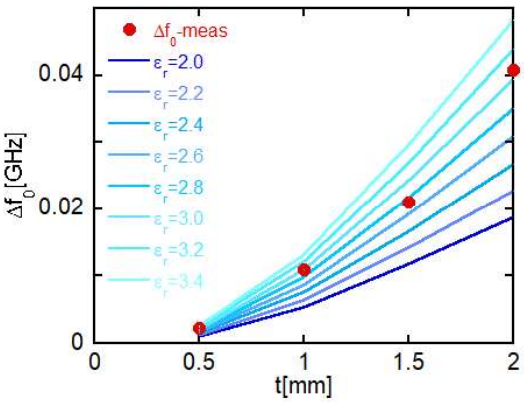

Figure 2 – Differences between the resonant frequencies $f_{0,S}$ with the samples mounted and $f_{0,A}$ with the sample substituted by an air gap of the same thickness. The red dots are the experimental data and the blue lines the simulations results.

Then, $\tan\delta_s$ is evaluated through Eq. (7) from the measured $\Delta[Q^{-1}] = Q_S^{-1} - Q_A^{-1}$. The quality factors Q are reported in Table 2.

Table 2 – The inverse of the measured quality factors when the four samples, S1-S4, are inserted. Q_S^{-1} and Q_A^{-1} refer to the measurement with the sample and an air gap of equal thickness, respectively.

	S_1	S_2	S_3	S_4
$Q_S^{-1} \cdot 10^4$	2.15	2.48	3.06	4.25
$Q_A^{-1} \cdot 10^4$	1.95	1.96	1.98	2.00

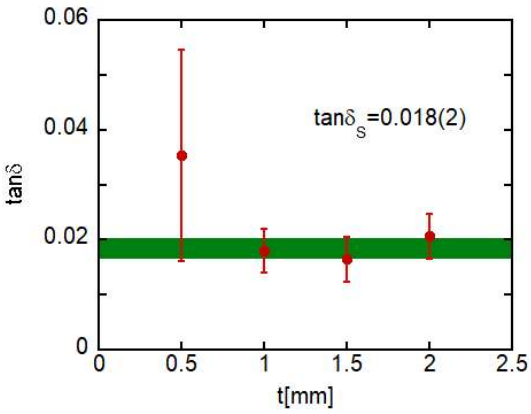

Figure 3 – The measured loss tangent of the dielectric 3D-printed material $\tan\delta_S$. The errors bar are evaluated with Eq.(8) and the green area represent the confidence interval.

The error bars of the experimental points in Figure 3 are evaluated with Eq. (8) using the uncertainties on the measured quantities and simulated parameter shown previously. Figure 3 shows the best $\tan\delta_S$ estimate, which comes out to be: $\tan\delta_S = (1.8 \pm 0.2) \cdot 10^{-2}$ as calculated with $\varepsilon_{r,S} = 2.9 \pm 0.2$. The evaluation of $\tan\delta_S$ is performed taking as best value the centre point in the common confidence interval of all the experimental points (the green band in Figure 3). Then, the uncertainty is the half width of that common interval. We note that the uncertainty bars rapidly increase when the sample thickness becomes small due to a lack of sensitivity: the method is a volume technique. This effect is present also in Figure 2, when the simulated curves for small thickness values tend to coalesce. On the contrary, samples with large thickness could cause e.m. field radiation from the structure, thus changing significantly the resonant mode and adding further losses. The method here presented, at our geometry, is then most suitable for samples of thickness between 1 and 2 mm.

IV. SUMMARY

We have presented a dielectric-resonator-based technique for the measurements of the complex permittivity of 3D printable materials. We exploited the possibility to shape the sample in appropriate shapes (disks, in our case) and the excellent frequency repeatability of our setup in order to reliably measure the quality factor and the resonance frequency, with and without the sample. The results yield an uncertainty of about 10 % on the loss tangent.

REFERENCES

[1] N. Hopkinson & P. Dickens, *Emerging Rapid Manufacturing Processes*, in Rapid Manufacturing: An industrial revolution for the digital age, Chichester, W. Sussex, Wiley&Sons Ltd, 2006.

[2] M. J. Werkheiser, J. Dunn, M. P. Snyder, J. Edmunson, K. Cooper & M. M. Johnston, *3D printing in Zero-G ISS technology demonstration.*, in AIAA SPACE 2014 Conference and Exposition, 2014.

[3] J. Y. Wong, *Ultra-portable solar-powered 3D printers for onsite manufacturing of medical resources*, Aerospace medicine and human performance, vol. 89, n. 9, pp. 830-834, 2015.

[4] C. Schubert, M. C. Van Langeveld & L. A. Donoso, *Innovations in 3D printing: a 3D overview from optics to organs*, British Journal of Ophthalmology, vol. 98, n. 2, pp. 159-161, 2014.

[5] F. Rengier, A. Mehndiratta, H. Von Tengg-Kobligk, C. M. Zechmann, R. Unterhinninghofen, H. Kauczor & F. L. Giesel, *3D printing based on imaging data: review of medical applications*, International journal of computer assisted radiology and surgery, vol. 5, n. 4, pp. 335-341, 2010.

[6] M. J. Burfeindt, T. J. Colgan, R. O. Mays, J. D. Shea, N. Behdad, B. D. Van Veen & S. C. Hagness, *MRI-derived 3-D-printed breast phantom for microwave breast imaging validation*., IEEE antennas and wireless propagation letters, vol. 11, pp. 1610-1613, 2012.

[7] Mobashsher, A. T., & Abbosh, A. M. *Three-dimensional human head phantom with realistic electrical properties and anatomy*. IEEE Antennas and Wireless Propagation Letters, vol. 13, pp. 1401-1404, 2014.

[8] Bisognin, A., Cihangir, A., Luxey, C., Jacquemod, G., Pilard, R., Gianesello, F., & Whittow, W. G., *Ball grid array-module with integrated shaped lens for WiGig applications in eyewear devices*, IEEE Transactions on Antennas and Propagation, vol. 64, n 3, pp. 872-882. 2016.

[9] Le Sage, G. P. *3D printed waveguide slot array antennas*. IEEE Access, vol. 4, pp. 1258-1265, 2016.

[10] Rashidian, A., Shafai, L., Sobocinski, M., Peräntie, J., Juuti, J., & Jantunen, H.. *Printable planar dielectric antennas*. IEEE Transactions on Antennas and Propagation, vol. 64, n. 2, pp. 403-413, 2016.

[11] Nayeri, P., Liang, M., Sabory-Garcı, R. A., Tuo, M., Yang, F., Gehm, M, & Elsherbeni, A. Z. *3D printed dielectric reflectarrays: low-cost high-gain antennas at sub-millimeter waves*. IEEE Transactions on Antennas and Propagation, vol. 62, n. 4, pp. 2000-2008, 2014.

[12] Garcia, C. R., Rumpf, R. C., Tsang, H. H., & Barton, J. H. *Effects of extreme surface roughness on 3D printed horn antenna*. Electronics Letters, vol. 49, n. 12, pp. 734-736, 2013.

[13] P. I. Deffenbaugh, R. C. Rumpf e K. H. Church, *Broadband microwave frequency characterization of 3-D printed materials*, IEEE Transactions on Components, Packaging and Manufacturing Technology, vol. 3, n. 12, pp. 2147-2155, 2013.

[14] L. F. Chen, C. K. Ong, C. P. Neo, V. V. Varadan and V. K. Varadan, Microwave electronics: measurement and materials characterization., John Wiley & Sons., 2004.

[15] Mazierska, J., & Wilker, C. *Accuracy issues in surface resistance measurements of high temperature superconductors using dielectric resonators (corrected)*. IEEE transactions on applied superconductivity, vol. 11, n. 4, pp. 4140-4147, 2001.

[16] Mazierska, J., & Jacob, M. V. *How Accurately Can the Surface Resistance of Various Superconducting Films Be Measured with the Sapphire Hakki–Coleman Dielectric Resonator Technique?*. Journal of superconductivity and novel magnetism, vol. 19, n. 7, pp. 649-655, 2006.

[17] F. Castles, D. Isakov, A. Lui, Q. Lei, C. E. J. Dancer, Y. Wang, J. M. Janurudin, S. C. Speller, C. R. M. Grovenor e P. S. Grant, *Microwave dielectric characterisation of 3D-printed $BaTiO_3$/ABS polymer composites*, Scientific reports, vol. 6, p. 22714, 2016.

[18] Felício, J. M., Fernandes, C. A., & Costa, J. R., *Complex permittivity and anisotropy measurement of 3D-printed PLA at microwaves and millimeter-waves,* in 2016 22nd International Conference on Applied Electromagnetics and Communications (ICECOM) (pp. 1-6). 2016.

[19] Hakki, B. W., & Coleman, P. D., *A dielectric resonator method of measuring inductive capacities in the millimeter range,* IRE Transactions on Microwave Theory and Techniques, vol. 8, n. 4, pp. 402-410, 1960.

[20] JCGM 100: Evaluation of Measurement Data – Guide to the Expression of Uncertainty in Measurement, 2008.

[21] Torokhtii, K., Alimenti, A., Pompeo, N., Leccese, F., Orsini, F., Scorza, A., Sciuto, S. A. & Silva, E., *Q-factor of microwave resonators: calibrated vs. uncalibrated measurements,* in Journal of Physics: Conference Series, Vol. 1065, No. 5, pp. 052027. IOP Publishing, 2018.

[22] Leong, K., & Mazierska, J., *Precise measurements of the Q factor of dielectric resonators in the transmission mode-accounting for noise, crosstalk, delay of uncalibrated lines, coupling loss, and coupling reactance*. IEEE Transactions on Microwave Theory and Techniques, vol. 50, n. 9, pp. 2115-2127, 2002.

[23] Pompeo, N., Torokhtii, K., Leccese, F., Scorza, A., Sciuto, S., & Silva, E., *Fitting strategy of resonance curves from microwave resonators with non-idealities*, in IEEE International Instrumentation and Measurement Technology Conference (I2MTC) (pp. 1-6). IEEE, 2017